Jpn J Ophthalmol (2013) 57:347–358
DOI 10.1007/s10384-013-0239-7

THE OFFICIAL INTERNATIONAL JOURNAL OF THE JAPANESE OPHTHALMOLOGICAL SOCIETY

CLINICAL INVESTIGATION

Comparison of two different spectral domain optical coherence tomography devices in the detection of localized retinal nerve fiber layer defects

Ko Eun Kim · Seong Joon Ahn · Dong Myung Kim

Received: 21 June 2012 / Accepted: 25 December 2012 / Published online: 29 March 2013

Abstract
Purpose To compare the detection of localized retinal nerve fiber layer (RNFL) defects by two different spectral domain optical coherence tomography (SD-OCT) devices.
Methods Eyes of 42 normal control subjects and 48 patients with a localized RNFL defect on red-free fundus photographs were imaged by the Cirrus (Carl Zeiss Meditec, Dublin, CA, USA) and 3D OCT (Topcon, Tokyo, Japan) devices. We compared sensitivities, specificities, and area under the receiver operating characteristic curves (AUCs) of circumpapillary RNFL (cpRNFL) thickness and ganglion cell complex (GCC) parameters between the two devices.
Results The devices provided different cpRNFL thickness measurements. The highest sensitivities at fixed specificities of 80 % (Cirrus: 83.3 %; 3D OCT: 77.1 %) and 95 % (Cirrus: 69.8 %; 3D OCT: 68.8 %) and the largest AUCs (Cirrus: 0.90; 3D OCT: 0.88) obtained by the cpRNFL parameters of the two devices were similar. Based on the internal normative database, the deviation-from-normal map of the Cirrus OCT device and the 36-segment map of the 3D OCT device had the highest sensitivity (89.6 and 91.7 %, respectively). Among the macular GCC parameters of the 3D OCT device, inferior macular RNFL thickness had the highest sensitivity (81.2 % at a specificity of 80 %) and the largest AUC (0.89).
Conclusions Although the two SD-OCT devices have different measurement protocols, they showed similar abilities for the detection of a localized RNFL defect.

Keywords Retinal nerve fiber layer defect · Cirrus OCT device · 3D OCT device · Sensitivity · Specificity

K. E. Kim · D. M. Kim (✉)
Department of Ophthalmology, Seoul National University Hospital, 28 Yongon-Dong, Chongno-Gu, Seoul 110-744, Korea
e-mail: dmkim@snu.ac.kr

S. J. Ahn
Department of Ophthalmology, Seoul National University Bundang Hospital, Seongnam, Korea

Introduction

Clinical evaluation of the retinal nerve fiber layer (RNFL) is essential for the diagnosis and follow-up of glaucoma because RNFL atrophy precedes optic disc damage and visual field defects in glaucoma [1, 2]. RNFL atrophy can be of two types: either localized or diffuse. The usefulness of optical coherence tomography (OCT) for the detection of RNFL atrophy has been well studied [3–8].

Time-domain OCT (TD-OCT) has a low sensitivity for identifying a localized RNFL defect in patients undergoing normal standard automated perimetry [6]. A new version of OCT, spectral-domain OCT (SD-OCT), has enhanced spatial resolution and faster image acquisition time. In addition, some SD-OCT devices provide a ganglion cell complex (GCC) thickness map that covers a square grid on the central macula [5, 7, 9]. The diagnostic power of GCC imaging may be comparable or complementary to circumpapillary RNFL (cpRNFL) imaging [7, 9–11]. Although SD-OCT was expected to allow improved detection of a localized RNFL defect using cpRNFL and macular GCC parameters, previous studies comparing the abilities of the Stratus OCT (Carl Zeiss Meditec, Dublin, CA, USA) and Cirrus OCT (Carl Zeiss Meditec) devices to detect a localized RNFL defect showed no significant difference [4, 12].

One comparative study showed that three different SD-OCT devices (Spectralis, Cirrus, and RTVue) had similar accuracies to detect glaucoma [13]. However, to the best of our knowledge, there has been no study that has compared the abilities of two or more different SD-OCT devices to detect localized RNFL defects. Kanamori et al. [14] reported that the thickness values obtained using the Cirrus OCT device were significantly smaller than those obtained using the 3D OCT device (Topcon, Tokyo, Japan), attributing these differences to the different measurement protocols of the two devices. Specifically, Cirrus OCT and 3D OCT have different optic disc circle scan diameters (3.46 vs. 3.4 mm, respectively), scan area (centered on the optic disc vs. centered on the optic disc or the fovea, respectively), analysis software, and ethnicity of normative database (Caucasians, Hispanic, Indians, and Africans vs. Japanese and Caucasians, respectively). As the differences between the two SD-OCT devices with regard to the measurement protocols and thickness values may affect their ability to detect RNFL atrophy, the aim of our study was to compare the Cirrus OCT and 3D OCT devices in the detection of a localized RNFL defect.

Materials and methods

Subjects and examinations

Subjects for this observational case–control study were recruited from Seoul National University Hospital. The study adhered to the tenets of the Declaration of Helsinki and was approved by the Institutional Review Board of Seoul National University Hospital. Informed consent was obtained from all participants.

All subjects had undergone complete ophthalmic examinations, including visual acuity measurement, autorefractometry, slit lamp biomicroscopy, Goldmann applanation tonometry, gonioscopy, dilated fundus examination, disc stereophotography, red-free fundus photography (VX-10; Kowa Optimed, Tokyo, Japan) and Swedish Interactive Threshold Algorithm (SITA) 30-2 perimetry (Humphrey Field Analyzer II; Carl Zeiss Meditec). Disc stereophotographs and red-free fundus photographs were taken with a digital fundus camera after maximum pupil dilation. Sixty-degree wide-angle views of the fundus that were carefully focused on the retina using a built-in split-line focusing device were obtained and reviewed on a LCD monitor.

Based on the red-free fundus photography findings, the subjects were assigned to either the localized RNFL defect group or the normal control group. A localized RNFL defect was defined as a well-outlined, dark wedge-shaped area in the brightly striated pattern of the surrounding healthy RNFL with its tip touching the optic disc border. Findings were evaluated independently by two trained ophthalmologists (SJA, KEK) in a masked fashion. When the first two experts disagreed, a third ophthalmologist (DMK) evaluated the photographs and the disagreement was resolved after discussion. For those patients for whom both eyes met the eligibility criteria, one eye was randomly chosen. The eye with a localized RNFL defect was selected for this study when one eye had a RNFL defect and the other was normal.

Inclusion criteria were a best-corrected visual acuity of 20/40 or better, a spherical equivalent between +5.00 and −5.00 D, and an open anterior chamber angle. Subjects with retinal abnormality, a history of retinal laser procedure, or neurologic diseases or who had undergone a previous intraocular surgery other than a cataract extraction were excluded. Subjects with a poor quality red-free fundus photograph or an unreliable visual field were also excluded. A visual field was considered to be reliable if the fixation losses were <20 %, the false-positive rate was <15 %, and the false-negative rate was <15 %.

Patients with a localized RNFL defect included those with perimetric glaucoma with corresponding visual field defects and those with preperimetric glaucoma with a normal visual field. The normal control group had an intraocular pressure (IOP) of ≤21 mmHg with no history of increased IOP, absence of glaucomatous disc appearance, no visible RNFL defect on the red-free RNFL photograph, and a normal standard automated perimetry result.

Optical coherence tomography

Optical coherence tomography imaging with the Cirrus HD-OCT model 4000 (software ver. 5.1.1.6; Carl Zeiss Meditec) and 3D OCT-2000 (software ver. 7.20; Topcon Medical Systems) devices was performed after pupil dilation in the patients and normal controls on the same day by one examiner.

Cirrus OCT was performed using the 6 × 6 × 2-mm optic disc cube mode, which obtains a series of 200 horizontal scan lines that are each composed of 200 A-scans × 1,024 axial pixels covering a 6 × 6-mm grid centered on the optic disc. The Cirrus OCT device uses an acquisition rate of 27,000 A-scans per second at an axial resolution of 5 μm. A 3.46-mm diameter calculation circle is automatically positioned around the optic disc, and the Cirrus OCT device extracts 256 A-scan samples along the path of the calculation circle from the data cube. To be included, all images had to have a signal strength of >6, good centering of the optic disc, and the absence of motion artifacts. Four-quadrant thicknesses (Fig. 1c-1), 12 clock-hour segment thicknesses (Fig. 1c-2), a global 360° average thickness, and a TSNIT thickness profile were obtained using the calculated cpRNFL thickness at each point along

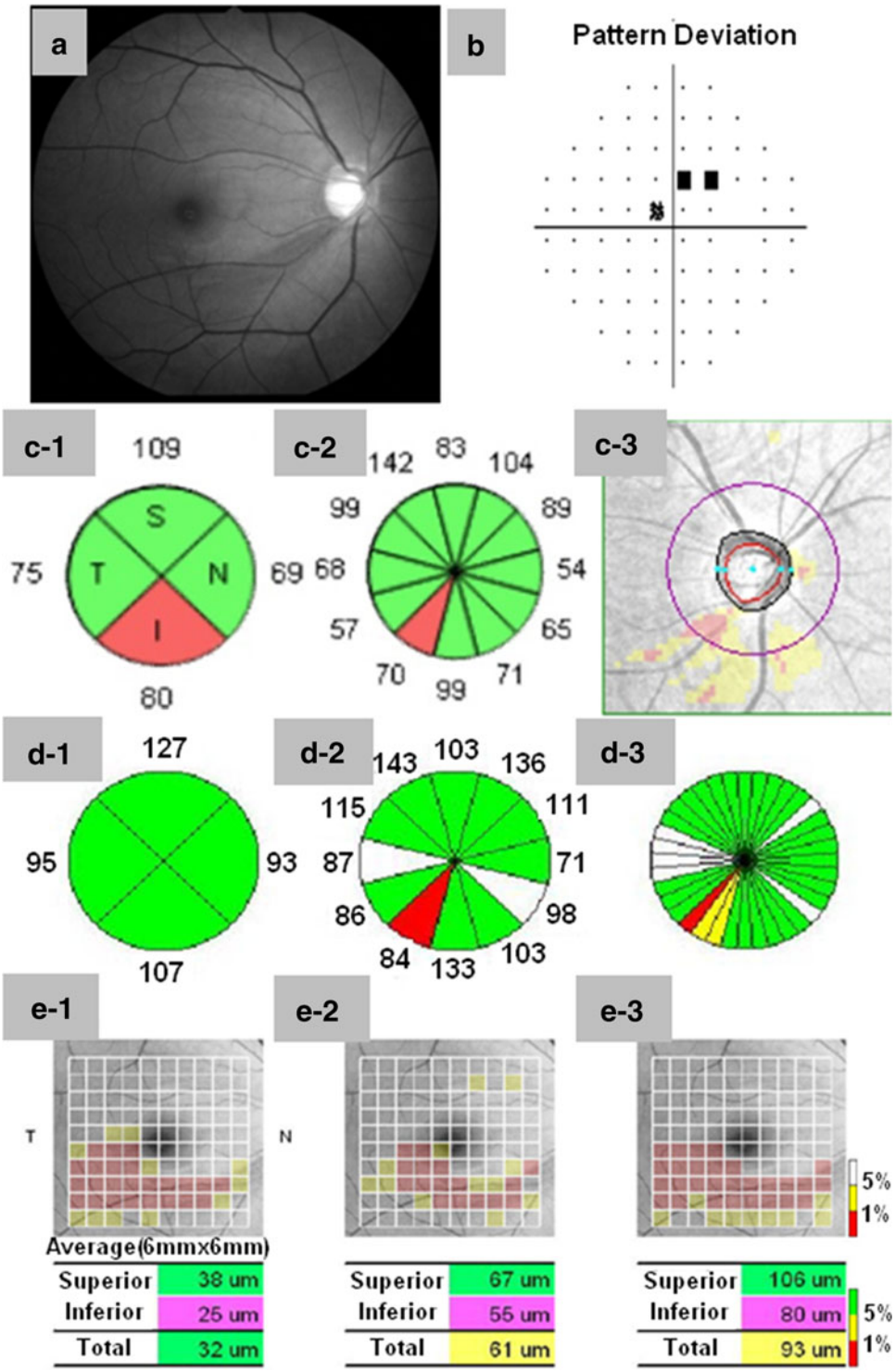

Fig. 1 Images of a right eye with a localized retinal nerve fiber layer (RNFL) defect. **a** Red-free fundus photography shows a localized RNFL defect in the inferior-temporal quadrant. **b** A pattern deviation map of the visual field shows defects corresponding to the RNFL defect. Optical coherence tomography (OCT) imaging with the Cirrus OCT device (Carl Zeiss Meditec, Dublin, CA, USA), circumpapillary RNFL thickness for quadrants (**c-1**) and clock-hour segments (**c-2**), and a deviation-from-normal map (**c-3**) show a corresponding RNFL defect. OCT imaging with the 3D OCT device (Topcon, Tokyo, Japan), circumpapillary RNFL thickness for clock-hour segments (**d-2**) and 36 segments (**d-3**), and thickness of macular RNFL (**e-1**), [ganglion cell layer (GCL) + inner plexiform layer (IPL)] (**e-2**), and [RNFL + GCL + IPL] (**e-3**) show a corresponding defect except for the circumpapillary RNFL thickness for quadrants (**d-1**)

the calculation circle. A deviation-from-normal map (Fig. 1c-3) derived from the superpixel average thickness measurement was also provided in the optic disc cube mode. RNFL thicknesses in the normal range were represented by green backgrounds, and those that were abnormal at the 5 and 1 % levels were represented by yellow and red, respectively.

The 3D OCT-2000 device has an axial scanning speed of 27,000 A-scans per second at an axial resolution of 5–6 μm, and the scanning protocol consisted of a circumpapillary scan and a macular cube scan (512 A-scans × 128 B-scans) covering an area of 6 × 6-mm centered on the fovea. The minimum acceptable Q factor score, which indicates quality of the image, was set at 60.

cpRNFL thickness was measured on a circle with a diameter of 3.4 mm centered on the optic disc. Thicknesses of four quadrants (Fig. 1d-1), 12 clock-hour segments (Fig. 1d-2), and 36 segments (Fig. 1d-3) and a TSNIT thickness profile were obtained. The results from the comparison of cpRNFL thickness with normative data were indicated with the same color scheme as in the Cirrus OCT. For macular GCC thickness, the built-in 3D OCT viewer computed the average thickness of the RNFL (Fig. 1e-1), [ganglion cell layer (GCL) + inner plexiform layer (IPL)] (Fig. 1e-2), and [RNFL + GCL + IPL] (Fig. 1e-3). The thickness values were also obtained in the superior and inferior hemiretina of the 6 × 6-mm square centered on the fovea.

A yellow or red display in quadrants, clock-hour segments, or 36 segments was defined as the detection of an RNFL defect when it corresponded to the clock-hour location of the RNFL defect observed on the red-free fundus photograph. A segment of the TSNIT thickness profile located below the yellow band (outside of the 95 % normal limit) and in the red band (outside of the 99 % normal limit) was defined as OCT RNFL defect at the 5 and 1 % level, respectively. If the OCT RNFL defect corresponded to the location of localized RNFL defect, we considered detection of the localized RNFL defect using TSNIT thickness profile.

Detection of a localized RNFL defect on the deviation-from-normal map of Cirrus OCT was defined when a wedge-shaped color pattern across a 3.46-mm calculation circle corresponding to the location on the red-free fundus photograph is represented by yellow or red display. A RNFL defect in the macular GCC images obtained by 3D OCT was defined as a wedge-shaped area that appeared to be less thick than neighboring areas corresponding to the location on the red-free photograph in color-coded maps of macular RNFL, [GCL + IPL], and [RNFL + GCL + IPL] thickness. At least four abnormal squares extending from the disc to the macula are required for the wedge-shaped defects in the maps.

Data analysis

In patients with two or more RNFL defects in one eye, the dominant RNFL defect was selected for data analysis. In the analysis of cpRNFL thickness of clock-hour segments, left eye data were converted into right eye format. For all quantitative data, Student's *t* test was used to compare RNFL thickness between eyes with a localized RNFL defect and normal control eyes. The agreement between RNFL measurements obtained by the two devices was investigated using Bland–Altman plots [15] in which the differences between measurements were plotted against their mean for each parameter. If the slope of the regression line between the two devices was statistically significant, we considered that a proportional bias existed, indicating that the difference in the RNFL thickness measurements between the two devices is a function of the RNFL thickness. Receiver operating characteristic (ROC) curves were built, and the area under the ROC curve (AUC) was calculated to evaluate the ability of each OCT parameter to differentiate patients with a RNFL defect from normal controls. The pairwise comparison of the AUCs was performed using a method proposed by DeLong et al. [16]. We also calculated sensitivities at fixed specificities (80 and 95 %) for each parameter. Sensitivities and specificities were tested on the basis of the comparison of measurements with a built-in normative database of the devices and calculated according to abnormalities at the 5 and 1 % levels. The AUCs, sensitivities at fixed specificities, and sensitivities and specificities based on internal normative database were separately analyzed in eyes with preperimetric and perimetric glaucoma.

Statistical analyses were performed using the Statistical Package for the Social Sciences (SPSS) for Windows (ver. 18.0; SPSS, Chicago, IL, USA) and the Bonferroni-adjusted significance level was used to reduce false positives attributable to multiple statistical tests. Thus, *P* values of <0.001, 0.05 divided by 50 (number of *P* values) were considered to be statistically significant, and *P* values between 0.001 and 0.05 were considered to be marginally significant. Commercially available software (Analyse-it; Analyse-it Software, Leeds, UK) was used to compare AUCs [17].

Results

During the enrollment period, this study initially included 94 eyes of 94 subjects (50 eyes with a localized RNFL defect and 44 normal control eyes). Four subjects (4.2 %) with unacceptable Cirrus or 3D OCT scans were excluded from further analyses, leaving 90 subjects (48 patients with a localized RNFL defect and 42 normal controls). In those with a RNFL defect, 34 eyes had perimetric glaucoma and 14 had preperimetric glaucoma. The demographics and ocular characteristics of the eyes are presented in Table 1. No significant differences with regard to the mean age, gender ratio, and spherical equivalent of refraction were observed between the two groups. However, the mean deviation and pattern standard deviation of the visual field were significantly different between the two groups. Forty-six patients had one localized RNFL defect and two patients had two localized RNFL defects, one in the superotemporal and the other in the inferotemporal quadrant. The frequency distribution of a localized RNFL defect in terms of clock-hour positions is shown in Fig. 2. The

Table 1 Demographics and ocular characteristics

Demographics and ocular characteristics	Normal eyes ($n = 42$)	Eyes with a localized RNFL defect ($n = 48$)	P value
Age, years	51.0 ± 12.7	55.4 ± 11.6	0.09[a]
Gender (M:F), n	17:25	18:30	0.92[b]
Intraocular pressure, mmHg	14.2 ± 3.3	15.7 ± 3.0	0.03[a]
Spherical equivalent, D	−0.9 ± 1.7	−1.4 ± 2.3	0.23[a]
Visual field			
Mean deviation, dB	−0.5 ± 1.4	−3.1 ± 3.3	<0.001[a]
Pattern standard deviation, dB	2.3 ± 1.1	5.3 ± 3.4	<0.001[a]

RNFL Retinal nerve fiber layer

Data are presented as the mean ± standard deviation, unless indicated otherwise

[a] Student's t test

[b] Chi-square test

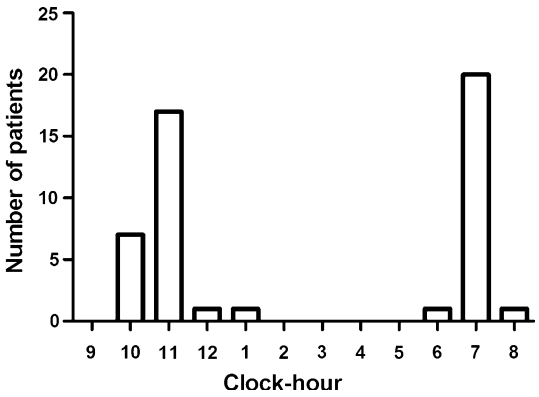

Fig. 2 Frequency distribution of localized RNFL defects in terms of clock-hour positions in 48 eyes with a localized RNFL defect on red-free fundus photographs

clock-hour positions of a localized RNFL defect in red-free fundus photographs coincided with OCT results in 77.1 and 75 % of eyes using the Cirrus OCT and 3D OCT devices, respectively.

RNFL thickness measurements, agreement of measurements, and AUC

Comparison of cpRNFL thickness measured by the Cirrus OCT device between normal eyes and eyes with a localized RNFL defect showed significant differences in the 12-, 11-, 8-, 7-, and 6-o'clock segments, superior and inferior quadrants, and average thickness. In the comparison of cpRNFL thickness measured by the 3D OCT device, significant differences between the two groups were observed in the 11-, 7-, and 6-o'clock segments, inferior quadrant, and average thickness. Comparison of the macular GCC parameters by the 3D OCT device showed that average thickness and superior and inferior thicknesses of the RNFL, [GCL + IPL], and [RNFL + GCL + IPL] had significantly decreased in those eyes with a localized RNFL defect. The mean thickness values of all cpRNFL parameters measured by the 3D OCT device were greater than those measured by the Cirrus OCT device (range of differences: 3.2–25.2 μm) (Table 2).

The correlation of thickness measurements between the two devices was statistically significant ($R^2 = 0.86$, $P < 0.001$), and the agreement of measurements between the two devices had a proportional bias on a Bland–Altman plot with marginal significance (slope of regression line: −0.16; $P = 0.015$).

Table 3 and Fig. 3 show the comparisons of the AUCs of the Cirrus OCT and 3D OCT parameters. The AUC values of cpRNFL thickness by the Cirrus OCT device were generally larger than those by the 3D OCT device, but the difference was not statistically significant for any parameter. Among the cpRNFL thickness parameters, the 7-o'clock segment had the largest AUC in both devices (Cirrus OCT: 0.90; 3D OCT: 0.88; $P = 0.56$). In the macular GCC parameters obtained by the 3D OCT, the inferior macular RNFL thickness, and average and inferior macular [RNFL + GCL + IPL] thicknesses had the largest AUCs (0.89). The largest AUCs for the macular GCC parameters (0.89) were not significantly different from those for the cpRNFL parameters (0.88) in the 3D OCT ($P = 0.79$). In addition, the largest AUCs were not significantly different between the two devices (Cirrus OCT: 0.90; 3D OCT: 0.89; $P = 0.80$) (Fig. 3). The AUCs for GCC parameters (range 0.73–0.89) were more similar than those for cpRNFL parameters (range 0.51–0.88). The AUCs in the comparisons between normal eyes and perimetric glaucoma eyes were generally larger than those between normal eyes and preperimetric glaucoma eyes (Table 3). In the comparison between normal eyes and perimetric glaucoma eyes, the Cirrus OCT and 3D OCT devices showed the largest AUCs (0.91 and 0.92, respectively) in the cpRNFL thickness of the 7-o'clock segment. In the comparison between normal eyes and preperimetric glaucoma eyes, the Cirrus OCT device showed the largest AUC in the cpRNFL thickness of the 7-o'clock segment and the 3D OCT device showed the largest AUC in the average and inferior thickness of [RNFL + GCL + IPL] (0.87 for both devices).

Sensitivities and specificities using thickness data and internal normative database

Table 4 provides sensitivities for specificities set at 95 % in the parameters measured by the Cirrus OCT and 3D

Table 2 Circumpapillary RNFL thicknesses by the Cirrus OCT and 3D OCT devices and macular ganglion cell complex thicknesses by the 3D OCT device in normal eyes and eyes with a localized RNFL defect

Parameters	Cirrus OCT device			3D OCT device		
	Normal eyes ($n = 42$)	Eyes with a localized RNFL defect ($n = 48$)	P value[a]	Normal eyes ($n = 42$)	Eyes with a localized RNFL defect ($n = 48$)	P value[a]
cpRNFL thickness, μm						
Average	93.1 ± 9.5	78.0 ± 10.8	<0.001	109.8 ± 13.2	95.5 ± 12.7	<0.001
Quadrant						
Superior	117.5 ± 18.1	96.0 ± 20.1	<0.001	131.4 ± 18.1	109.1 ± 24.8	0.001
Nasal	66.8 ± 8.1	63.4 ± 7.6	0.043	88.3 ± 21.8	82.7 ± 16.9	0.172
Inferior	119.4 ± 16.1	90.8 ± 22.4	<0.001	132.7 ± 24.5	109.4 ± 23.0	<0.001
Temporal	68.8 ± 10.2	61.7 ± 11.7	0.003	85.0 ± 14.0	81.1 ± 21.0	0.305
Clock-hour segment						
12	119.5 ± 29.0	96.9 ± 27.9	<0.001	128.6 ± 27.2	109.9 ± 24.9	0.001
11	125.0 ± 19.9	96.4 ± 25.8	<0.001	138.2 ± 20.7	111.6 ± 28.9	<0.001
10	78.8 ± 12.9	71.7 ± 16.7	0.029	100.2 ± 21.5	90.8 ± 19.9	0.036
9	55.6 ± 7.6	54.7 ± 9.5	0.605	71.7 ± 13.5	71.6 ± 13.6	0.976
8	71.4 ± 13.8	58.6 ± 12.6	<0.001	83.9 ± 16.2	75.4 ± 17.3	0.018
7	139.4 ± 19.7	87.5 ± 30.0	<0.001	142.6 ± 19.5	96.6 ± 28.7	<0.001
6	125.8 ± 23.5	101.4 ± 30.6	<0.001	146.3 ± 19.5	123.2 ± 32.0	<0.001
5	93.2 ± 21.3	83.5 ± 21.2	0.035	118.4 ± 23.8	108.7 ± 27.4	0.08
4	63.5 ± 10.8	56.6 ± 9.5	0.069	83.6 ± 24.5	80.2 ± 17.1	0.441
3	58.8 ± 7.6	57.0 ± 7.2	0.263	76.3 ± 22.3	75.9 ± 24.0	0.94
2	78.3 ± 12.0	72.6 ± 11.7	0.027	101.3 ± 25.4	93.2 ± 22.6	0.114
1	107.9 ± 23.6	94.0 ± 24.0	0.007	127.1 ± 23.7	111.8 ± 24.1	0.003
Macular ganglion cell complex						
Thickness of RNFL, μm						
Average	N/A	N/A	N/A	36.9 ± 4.2	28.1 ± 6.3	<0.001
Superior	N/A	N/A	N/A	35.5 ± 4.0	30.5 ± 6.6	<0.001
Inferior	N/A	N/A	N/A	38.4 ± 5.1	25.8 ± 9.2	<0.001
Thickness of [GCL + IPL], μm						
Average	N/A	N/A	N/A	68.3 ± 4.3	62.2 ± 5.5	<0.001
Superior	N/A	N/A	N/A	69.7 ± 4.5	64.6 ± 5.9	<0.001
Inferior	N/A	N/A	N/A	67.0 ± 4.4	60.0 ± 6.3	<0.001
Thickness of [RNFL + GCL + IPL], μm						
Average	N/A	N/A	N/A	105.3 ± 7.0	90.1 ± 10.6	<0.001
Superior	N/A	N/A	N/A	105.1 ± 6.7	94.4 ± 11.9	<0.001
Inferior	N/A	N/A	N/A	105.4 ± 7.9	85.7 ± 13.5	<0.001

cpRNFL Circumpapillary retinal nerve fiber layer, *GCL* ganglion cell layer, *IPL* inner plexiform layer, *N/A* not applicable

[a] P value according to Student's t test

OCT devices. In general, sensitivities at the fixed specificities were similar between the two devices. cpRNFL thickness of the 7-o'clock segment had the highest sensitivity (83.3 and 69.8 % at fixed specificities of 80 and 95 %, respectively) for the Cirrus OCT, whereas inferior macular RNFL thickness had the highest sensitivity (81.2 and 70.2 % at fixed specificities of 80 and 95 %, respectively) for the 3D OCT. In both preperimetric and perimetric glaucoma, cpRNFL thickness of the 7-o'clock segment for the Cirrus OCT device and inferior macular RNFL thickness for the 3D OCT device showed the highest sensitivity.

We obtained sensitivities and specificities for the cpRNFL thickness and macular GCC parameters from the internal normative database (Table 5). With regard to the cpRNFL thickness parameters, the sensitivities and specificities of the 3D OCT device were comparable to those of the Cirrus OCT device. However, for the Cirrus OCT

Table 3 Area under receiver operating characteristic curves for the Cirrus OCT and 3D OCT parameters

Parameters	Normal eyes ($n = 42$) vs. eyes with a localized RNFL defect ($n = 48$)			Normal eyes ($n = 42$) vs. preperimetric glaucoma eyes ($n = 14$)		Normal eyes ($n = 42$) vs. perimetric glaucoma eyes ($n = 34$)	
	Cirrus OCT device	3D OCT device	P[a]	Cirrus OCT device	3D OCT device	Cirrus OCT device	3D OCT device
cpRNFL thickness							
Average	0.85 (0.77–0.93)	0.78 (0.69–0.88)	0.03	0.81 (0.68–0.94)	0.71 (0.56–0.87)	0.87 (0.78–0.96)	0.87 (0.78–0.96)
Quadrant							
Superior	0.80 (0.70–0.89)	0.78 (0.68–0.87)	0.43	0.72 (0.58–0.86)	0.70 (0.53–0.86)	0.82 (0.72–0.93)	0.82 (0.72–0.93)
Nasal	0.63 (0.51–0.74)	0.56 (0.44–0.68)	0.18	0.62 (0.44–0.79)	0.54 (0.36–0.71)	0.63 (0.50–0.75)	0.63 (0.50–0.75)
Inferior	0.83 (0.75–0.92)	0.80 (0.71–0.89)	0.32	0.80 (0.68–0.92)	0.76 (0.61–0.91)	0.84 (0.75–0.94)	0.84 (0.75–0.94)
Temporal	0.71 (0.60–0.82)	0.62 (0.50–0.74)	0.04	0.74 (0.61–0.87)	0.60 (0.43–0.78)	0.69 (0.56–0.81)	0.69 (0.56–0.81)
Clock-hour segment							
12	0.73 (0.63–0.84)	0.70 (0.59–0.81)	0.33	0.62 (0.47–0.76)	0.58 (0.42–0.75)	0.77 (0.66–0.89)	0.75 (0.63–0.86)
11	0.80 (0.71–0.89)	0.77 (0.68–0.87)	0.54	0.75 (0.61–0.88)	0.69 (0.50–0.88)	0.82 (0.72–0.91)	0.80 (0.70–0.90)
10	0.65 (0.53–0.76)	0.62 (0.51–0.74)	0.64	0.71 (0.56–0.86)	0.67 (0.49–0.84)	0.61 (0.48–0.75)	0.61 (0.48–0.74)
9	0.55 (0.43–0.67)	0.51 (0.39–0.64)	0.57	0.56 (0.37–0.75)	0.57 (0.40–0.75)	0.54 (0.40–0.67)	0.48 (0.34–0.61)
8	0.77 (0.67–0.87)	0.66 (0.54–0.77)	0.03	0.74 (0.61–0.87)	0.55 (0.36–0.74)	0.78 (0.67–0.89)	0.70 (0.57–0.83)
7	**0.90** (0.83–0.97)	0.88 (0.82–0.95)	0.56	**0.87** (0.74–1.00)	0.82 (0.68–0.95)	**0.91** (0.84–0.99)	**0.92** (0.85–0.98)
6	0.73 (0.63–0.84)	0.72 (0.61–0.82)	0.62	0.58 (0.40–0.76)	0.59 (0.41–0.78)	0.80 (0.69–0.91)	0.76 (0.65–0.88)
5	0.63 (0.52–0.75)	0.62 (0.50–0.74)	0.75	0.58 (0.40–0.75)	0.61 (0.42–0.79)	0.66 (0.53–0.78)	0.62 (0.49–0.75)
4	0.60 (0.48–0.72)	0.54 (0.42–0.67)	0.37	0.66 (0.49–0.83)	0.57 (0.40–0.74)	0.58 (0.45–0.71)	0.54 (0.41–0.67)
3	0.57 (0.45–0.69)	0.51 (0.39–0.63)	0.37	0.61 (0.45–0.78)	0.48 (0.29–0.67)	0.55 (0.41–0.68)	0.52 (0.39–0.66)
2	0.64 (0.52–0.75)	0.59 (0.47–0.71)	0.30	0.52 (0.34–0.70)	0.53 (0.37–0.69)	0.68 (0.56–0.80)	0.60 (0.47–0.73)
1	0.67 (0.56–0.78)	0.67 (0.56–0.78)	1.00	0.60 (0.43–0.78)	0.61 (0.44–0.77)	0.70 (0.57–0.82)	0.70 (0.58–0.82)
Macular ganglion cell complex							
Thickness of RNFL							
Average	N/A	0.88 (0.81–0.95)	N/A	N/A	0.87 (0.78–0.95)	N/A	0.91 (0.82–1.00)
Superior	N/A	0.73 (0.62–0.83)	N/A	N/A	0.69 (0.57–0.81)	N/A	0.81 (0.67–0.95)
Inferior	N/A	**0.89** (0.81–0.96)	N/A	N/A	0.87 (0.78–0.96)	N/A	0.91 (0.80–1.00)
Thickness of [GCL + IPL]							
Average	N/A	0.81 (0.72–0.90)	N/A	N/A	0.78 (0.64–0.92)	N/A	0.82 (0.72–0.92)
Superior	N/A	0.77 (0.67–0.87)	N/A	N/A	0.75 (0.59–0.92)	N/A	0.78 (0.66–0.89)
Inferior	N/A	0.82 (0.73–0.91)	N/A	N/A	0.79 (0.65–0.93)	N/A	0.83 (0.73–0.93)
Thickness of [RNFL + GCL + IPL]							
Average	N/A	**0.89** (0.82–0.96)	N/A	N/A	**0.89** (0.81–0.97)	N/A	0.90 (0.81–1.00)
Superior	N/A	0.77 (0.67–0.86)	N/A	N/A	0.81 (0.67–0.95)	N/A	0.75 (0.63–0.87)
Inferior	N/A	**0.89** (0.81–0.96)	N/A	N/A	**0.89** (0.77–1.00)	N/A	0.89 (0.80–0.97)

The largest area under the receiver operating characteristic (ROC) curves for each device is given in bold

Value in parenthesis is the 95 % confidence interval (CI)

[a] Comparison was performed using the method of DeLong et al. [16]

device, the deviation-from-normal map had the highest sensitivity (89.6 %) and for the 3D OCT device, the 36-segment map and TSNIT thickness profile had the highest sensitivity (91.7 %). These parameters also showed the highest sensitivities in eyes with preperimetric and perimetric glaucoma. For the 3D OCT device, the 36-segment map had a higher sensitivity than the clock-hour segment (91.7 vs. 75 % at the 5 % level) without significantly affecting specificity (81.0 vs. 85.7 % at the 5 % level) in detecting a localized RNFL defect. Sensitivities and specificities at the 5 and 1 % levels of the 36-segment map for the 3D OCT device were similar to those of the deviation-from-normal map for the Cirrus OCT device.

For macular GCC, the highest sensitivity and specificity was obtained when macular RNFL thickness was used. Macular RNFL thickness showed sensitivities of 85.4 and 68.8 % and specificities of 97.6 and 97.6 % at the 5 and

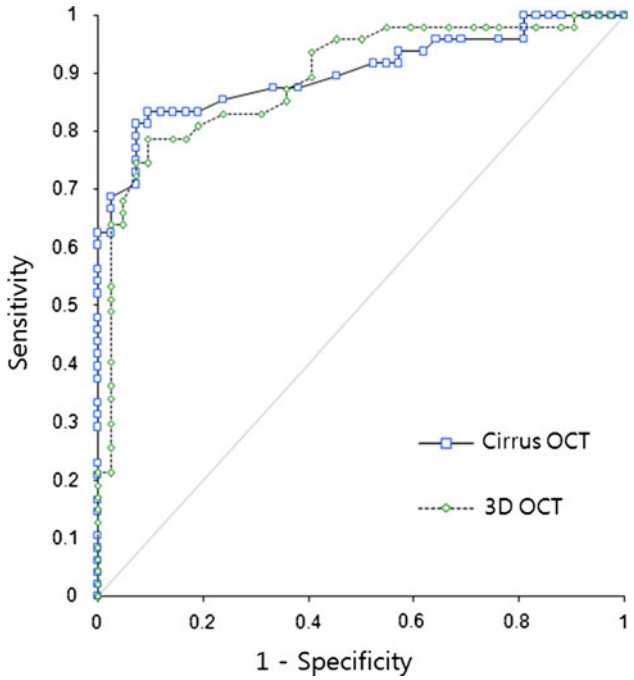

Fig. 3 Comparison of the largest area under receiver operating characteristic curves for the parameters measured by the Cirrus OCT and 3D OCT devices. Areas under receiver operating characteristic curve for the 7-o'clock segment of the circumpapillary retinal nerve fiber layer thickness measured by the Cirrus OCT device and average thickness of macular [RNFL + GCL + IPL] measured by the 3D OCT device were not significantly different ($P = 0.80$)

1 % levels, respectively. These values were comparable to those obtained from the deviation-from-normal map for the Cirrus OCT device (89.6 and 77.1 % sensitivities and 88.1 and 95.2 % specificities at the 5 and 1 % levels, respectively).

Discussion

The results of this study show that the Cirrus OCT and 3D OCT devices have similar abilities for the detection of a localized RNFL defect. In earlier studies evaluating the diagnostic performance of the Cirrus OCT device, the parameter that provided the largest AUC varied [4, 5, 13, 18–20]. Our results are similar to those of Jeoung et al. [4] and Park et al. [19], who report that, for the Cirrus OCT device, cpRNFL thickness of the average, inferior quadrant, and 7-o'clock segment were the best parameters for detecting a localized RNFL defect. The AUCs have varied in different studies of different study populations because differences in the disease severity of a specific population contributes to the variation in diagnostic accuracies; for example, the study of Park et al. [19] that included eyes with perimetric glaucoma showed a larger AUC (0.95) than that of Jeoung et al. [4] which included eyes with preperimetric glaucoma (0.73). The association between disease severity and diagnostic accuracies was also noted in our study; the largest AUC between normal and preperimetric glaucoma eyes (0.87) was smaller than that between normal and perimetric glaucoma eyes (0.91) using the Cirrus OCT device. For this reason, we separately analyzed the indicators of diagnostic abilities, namely, sensitivities, specificities, and AUCs, in eyes with preperimetric and perimetric glaucoma to compare our results with previous ones. Consequently, the AUC between normal and perimetric glaucoma eyes is similar in Park et al.'s study (0.95) and our study (0.92) but that between normal and preperimetric glaucoma eyes differs between Jeoung et al.'s study (0.73) and our study (0.87). As the number of preperimetric glaucoma patients enrolled in our study is small ($n = 14$), selection bias might have affected the AUC in our study. Furthermore, AUCs for cpRNFL thicknesses might be affected by ocular rotation [21], which can be another source of difference, but this parameter was not assessed in our study.

For the 3D OCT, the parameters with the largest AUCs were inferior macular RNFL thickness, average thickness of [RNFL + GCL + IPL], and inferior thickness of [RNFL + GCL + IPL] for the detection of a localized defect. In a previous study by Kotera et al. [22], the largest AUC between normal and preperimetric glaucoma was obtained for the inferior temporal outer sector of [RNFL + GCL + IPL] (0.86), but this parameter was not evaluated in our study. Instead, our results showed that average or inferior thickness of [RNFL + GCL + IPL] had the largest AUC (0.89) between normal and preperimetric glaucoma eyes. In another study using the 3D OCT device, the AUC of average macular RNFL thickness between the normal and perimetric glaucoma group was 0.896 [7], and a similar result was obtained in our study (0.91). The results of these previous studies on preperimetric and perimetric glaucoma groups are similar to our results.

The values of cpRNFL thickness from the two devices were different and showed proportional bias. The presence of proportional bias suggests that the different RNFL thickness measurements obtained by the different devices vary according to the actual measurement [23]. Earlier studies on the RNFL thickness showed that measurements obtained from the Cirrus OCT were thinner than those obtained from the 3D OCT in both normal eyes and those with a localized RNFL defect, and there was a strong proportional bias between the two measurements [14, 24], which is compatible with our result. Our study also shows that the difference of thickness between normal eyes and those with a localized RNFL defect in each cpRNFL parameter was greater in the Cirrus OCT than in the 3D OCT (Table 3). For example, the cpRNFL thickness

Table 4 Sensitivities for specificities set at 95 % for the Cirrus OCT and 3D OCT parameters

Parameters	Normal eyes ($n = 42$) vs. eyes with a localized RNFL defect ($n = 48$)		Normal eyes ($n = 42$) vs. preperimetric glaucoma eyes ($n = 14$)		Normal eyes ($n = 42$) vs. perimetric glaucoma eyes ($n = 34$)	
	Cirrus OCT device (%)	3D OCT device (%)	Cirrus OCT device (%)	3D OCT device (%)	Cirrus OCT device (%)	3D OCT device (%)
cpRNFL thickness						
Average	62.5	41.7	33.3	38.1	47.6	38.1
Quadrant						
Superior	41.7	33.3	38.1	23.8	42.9	28.6
Nasal	12.5	18.8	9.5	16.7	16.7	16.7
Inferior	56.3	48.0	52.4	57.1	57.1	52.4
Temporal	20.8	20.8	23.8	16.7	23.8	18.2
Clock-hour segment						
12	18.8	14.6	16.7	11.9	28.6	16.7
11	41.7	47.9	31.0	16.7	42.9	38.1
10	20.8	18.8	19.0	11.9	19.0	11.9
9	12.5	4.2	4.8	2.4	4.8	2.4
8	29.2	25.0	28.6	21.4	28.6	21.4
7	**69.8**	68.8	**54.8**	47.6	**66.7**	64.3
6	50.0	41.7	23.8	21.4	35.7	28.6
5	18.8	14.6	16.7	14.3	21.4	15.2
4	10.4	14.6	9.5	16.7	16.7	16.7
3	10.4	8.3	9.5	4.8	9.5	4.8
2	20.8	18.8	11.9	7.1	16.7	16.7
1	18.8	20.8	14.3	19.0	23.8	21.4
Macular ganglion cell complex						
Thickness of RNFL						
Average	N/A	70.2	N/A	52.4	N/A	66.7
Superior	N/A	42.6	N/A	40.5	N/A	40.5
Inferior	N/A	**70.2**	N/A	**64.3**	N/A	**64.3**
Thickness of [GCL + IPL]						
Average	N/A	53.2	N/A	38.1	N/A	52.4
Superior	N/A	40.4	N/A	26.2	N/A	40.5
Inferior	N/A	53.2	N/A	40.5	N/A	40.5
Thickness of [RNFL + GCL + IPL]						
Average	N/A	63.8	N/A	50.0	N/A	64.3
Superior	N/A	51.1	N/A	33.3	N/A	33.3
Inferior	N/A	70.2	N/A	54.8	N/A	54.8

The greatest sensitivity for each device is given in bold

difference of the inferior quadrant between normal eyes and those with a localized RNFL defect was 28.6 and 23.3 μm in the Cirrus OCT and 3D OCT, respectively. In our study, despite of the RNFL thickness differences and proportional bias, the two devices had similar abilities to detect a localized RNFL defect. However, future studies should include larger population to investigate whether RNFL thickness differences and proportional bias affect the diagnostic accuracies of the two SD-OCT devices.

According to the internal normative database, the parameter with the highest sensitivity using the Cirrus OCT device was obtained with the deviation-from-normal map (89.6 at the 5 % level), whereas with the 3D OCT device the parameter with the highest sensitivity was obtained with the TSNIT thickness profile and the 36-segment map (91.7 at the 5 % level). To the best of our knowledge, this is the first study reporting the diagnostic accuracies of the 36-segment map for the detection of a localized RNFL defect. Sensitivities were also similar at the 1 % level for the 36-segment map of the 3D OCT device and the deviation-from-normal map of the Cirrus OCT device (75.0 and 77.1 %, respectively). In a previous study, the optical

Table 5 Sensitivities and specificities (95 % CI) for the Cirrus OCT and 3D OCT parameters based on the internal normative database

Parameters	Normal eyes ($n = 42$) vs. eyes with a localized RNFL defect ($n = 48$)				Normal eyes ($n = 42$) vs. preperimetric glaucoma eyes ($n = 14$)		Normal eyes ($n = 42$) vs. perimetric glaucoma eyes ($n = 34$)	
	Cirrus OCT device		3D OCT device		Cirrus OCT device	3D OCT device	Cirrus OCT device	3D OCT device
	Sensitivity, %	Specificity, %	Sensitivity, %	Specificity, %	Sensitivity, %	Sensitivity, %	Sensitivity, %	Sensitivity, %
cpRNFL thickness								
≥1 clock-hour								
5 % level	77.1 (62.7–88.0)	78.6 (63.2–89.7)	75.0 (60.4–86.4)	85.7 (71.5–94.6)	42.9 (17.7–71.1)	57.1 (28.9–82.3)	91.2 (76.3–98.1)	82.4 (65.5–93.2)
1 % level	52.1 (37.2–66.7)	95.2 (83.8–99.4)	58.3 (43.2–72.4)	92.9 (80.5–98.5)	21.4 (4.7–50.8)	28.6 (8.4–58.1)	64.7 (46.5–80.3)	70.6 (52.5–84.9)
≥1 Quadrant								
5 % level	66.7 (51.6–79.6)	83.3 (68.6–93.0)	43.8 (29.5–58.8)	97.6 (87.4–99.9)	28.6 (8.4–58.1)	7.1 (0.2–33.9)	82.4 (65.5–93.2)	58.8 (40.7–75.4)
1 % level	52.1 (37.2–66.7)	95.2 (83.8–99.4)	20.8 (10.5–35.0)	100 (91.6–100)	21.4 (4.7–50.8)	0 (0–23.2)	67.7 (49.5–82.6)	29.4 (15.1–47.5)
≥1 out of 36 segments								
5 % level	N/A	N/A	**91.7** (80.0–97.7)	81.0 (65.9–91.4)	N/A	78.6 (49.2–95.3)	N/A	**97.1** (84.7–100.0)
1 % level	N/A	N/A	75.0 (60.4–86.4)	92.9 (80.5–98.5)	N/A	50.0 (23.0–77.0)	N/A	85.3 (68.9–95.0)
Average								
5 % level	52.1 (37.2–66.7)	92.9 (80.5–98.5)	N/A	N/A	35.7 (12.8–64.9)	N/A	58.8 (40.7–75.4)	N/A
1 % level	29.2 (17.0–44.1)	100 (91.6–100)	N/A	N/A	7.1 (0.2–33.9)	N/A	38.2 (22.2–56.4)	N/A
TSNIT thickness profile								
5 % level	87.5 (74.8–95.3)	78.6 (63.2–89.7)	**91.7** (80.0–97.7)	85.7 (71.5–94.6)	71.4 (41.9–91.6)	**85.7** (57.2–98.2)	94.1 (80.3–99.3)	94.1 (80.3–99.3)
1 % level	70.8 (55.9–83.0)	95.2 (83.8–99.4)	64.6 (49.5–77.8)	97.6 (87.4–99.9)	50.0 (23.0–77.0)	50.0 (23.0–77.0)	79.4 (62.1–91.3)	70.6 (52.5–84.9)
Deviation-from-normal map								
5 % level	**89.6** (77.3–96.5)	88.1 (74.4–96.0)	N/A	N/A	**71.4** (41.9–91.6)	N/A	**97.1** (84.7–99.9)	N/A
1 % level	77.1 (62.7–88.0)	95.2 (83.8–99.4)	N/A	N/A	57.1 (28.9–82.3)	N/A	85.3 (68.9–95.0)	N/A
Macular ganglion cell complex								
Thickness of RNFL								
5 % level	N/A	N/A	85.4 (72.2–93.9)	97.6 (87.4–99.9)	N/A	78.6 (49.2–95.3)	N/A	87.9 (71.8–96.6)
1 % level	N/A	N/A	68.8 (53.7–81.3)	97.6 (87.4–99.9)	N/A	64.3 (35.1–87.2)	N/A	72.7 (54.5–86.7)
Thickness of [GCL + IPL]								
5 % level	N/A	N/A	62.5 (47.4–76.0)	88.1 (74.4–96.0)	N/A	50.0 (23.0–77.0)	N/A	69.7 (51.3–84.4)
1 % level	N/A	N/A	47.9 (33.3–62.8)	95.2 (83.8–99.4)	N/A	42.9 (17.7–71.1)	N/A	51.5 (33.5–69.2)
Thickness of [RNFL + GCL + IPL]								
5 % level	N/A	N/A	64.6 (49.5–77.8)	97.6 (87.4–99.9)	N/A	57.1 (28.9–82.3)	N/A	69.7 (51.3–84.4)
1 % level	N/A	N/A	45.8 (31.4–60.8)	97.6 (87.4–99.9)	N/A	42.9 (17.7–71.1)	N/A	48.5 (30.8–66.5)

The greatest sensitivities for each device are given in bold

Specificities of the 3D OCT and Cirrus OCT parameters in normal eyes vs. preperimetric glaucoma eyes and normal eyes vs. perimetric glaucoma eyes are identical with those obtained by normal eyes vs. eyes with a localized RNFL defect analyses. For this reason, to avoid repetition of the results, the data on sensitivities are only presented

Value in parenthesis is the 95 % CI

cutoff point for the angle width of a RNFL defect was 10.69° on the deviation-from-normal map [5]. Since one segment in the 36-segment map of the 3D OCT device covers 10°, the cutoff point is expected to be close to that of the deviation-from-normal map of the Cirrus OCT device (10.69°). This might explain the similar sensitivities between the two maps of the devices. In addition, sensitivities of the deviation-from-normal map of the Cirrus OCT device were similar to those of the macular RNFL thickness map of the 3D OCT device (sensitivity of 85.4 % at the 5 % level). The two maps demonstrated morphologically similar wedge-shaped RNFL defects that correspond to observations made on the red-free fundus photographs, which might result in similar sensitivities.

The RNFL, GCL, and IPL of the retina are known to be affected in glaucoma, however, the outer retinal layers are largely not affected [11]. The AUCs between macular RNFL thickness only and thickness of [RNFL + GCL + IPL] were comparable, which suggest that AUCs of the macular GCC parameters are more dependent on the macular RNFL thickness than on the thickness of [GCL + IPL] and that glaucomatous damage might be more noticeable in the RNFL than in the other two layers.

This study has several limitations that warrant consideration. Only a small number of participants with preperimetric glaucoma were included in this study, which makes it hard to draw any conclusions on preperimetric glaucoma eyes. Therefore, a larger number of patients with preperimetric glaucoma should be included in future studies. In addition, data on macular parameters could not be obtained using the Cirrus OCT device. A comparison of macular parameters between the two SD-OCT devices was not possible, which necessitates further studies on the comparison of macular parameters. Furthermore, generalization of the AUCs and sensitivities/specificities from this study to all glaucoma patients is limited because approximately 25 % of patients with glaucoma have purely localized RNFL defects [25].

In conclusion, this study shows that the Cirrus OCT and 3D OCT devices had similar abilities for the detection of a localized RNFL defect, even though they differed in the measurement protocols and values for RNFL thickness.

Acknowledgments All authors had full access to all the data in the study and take responsibility for the integrity of the data and the accuracy of the data analysis. This work was supported by Grant number 3020110090 from the Seoul National University Hospital Research Fund donated by Mr. Bong Joo Kim.

References

1. Sommer A, Katz J, Quigley HA, Miller NR, Robin AL, Richter RC, et al. Clinically detectable nerve fiber atrophy precedes the onset of glaucomatous field loss. Arch Ophthalmol. 1991;109:77–83.
2. Tuulonen A, Lehtola J, Airaksinen PJ. Nerve fiber layer defects with normal visual fields. Do normal optic disc and normal visual field indicate absence of glaucomatous abnormality? Ophthalmology. 1993;100:587–97.
3. Jeoung JW, Kim SH, Park KH, Kim TW, Kim DM. Quantitative assessment of diffuse retinal nerve fiber layer atrophy using optical coherence tomography: diffuse atrophy imaging study. Ophthalmology. 2010;117:1946–52.
4. Jeoung JW, Park KH. Comparison of Cirrus OCT and Stratus OCT on the ability to detect localized retinal nerve fiber layer defects in preperimetric glaucoma. Invest Ophthalmol Vis Sci. 2010;51:938–45.
5. Seong M, Sung KR, Choi EH, Kang SY, Cho JW, Um TW, et al. Macular and peripapillary retinal nerve fiber layer measurements by spectral domain optical coherence tomography in normal-tension glaucoma. Invest Ophthalmol Vis Sci. 2010;51:1446–52.
6. Kim TW, Park UC, Park KH, Kim DM. Ability of Stratus OCT to identify localized retinal nerve fiber layer defects in patients with normal standard automated perimetry results. Invest Ophthalmol Vis Sci. 2007;48:1635–41.
7. Sakamoto A, Hangai M, Nukada M, Nakanishi H, Mori S, Kotera Y, et al. Three-dimensional imaging of the macular retinal nerve fiber layer in glaucoma with spectral-domain optical coherence tomography. Invest Ophthalmol Vis Sci. 2010;51:5062–70.
8. Manassakorn A, Aupapong S. Retinal nerve fiber layer defect patterns in primary angle-closure and open-angle glaucoma: a comparison using optical coherence tomography. Jpn J Ophthalmol. 2011;55:28–34.
9. Tan O, Chopra V, Lu AT, Schuman JS, Ishikawa H, Wollstein G, et al. Detection of macular ganglion cell loss in glaucoma by Fourier-domain optical coherence tomography. Ophthalmology. 2009;116:2305–14.
10. Ishikawa H, Stein DM, Wollstein G, Beaton S, Fujimoto JG, Schuman JS. Macular segmentation with optical coherence tomography. Invest Ophthalmol Vis Sci. 2005;46:2012–7.
11. Tan O, Li G, Lu AT, Varma R, Huang D. Mapping of macular substructures with optical coherence tomography for glaucoma diagnosis. Ophthalmology. 2008;115:949–56.
12. Sehi M, Grewal DS, Sheets CW, Greenfield DS. Diagnostic ability of Fourier-domain vs time-domain optical coherence tomography for glaucoma detection. Am J Ophthalmol. 2009;148:597–605.
13. Leite MT, Rao HL, Zangwill LM, Weinreb RN, Medeiros FA. Comparison of the diagnostic accuracies of the Spectralis, Cirrus, and RTVue optical coherence tomography devices in glaucoma. Ophthalmology. 2011;118:1334–9.
14. Kanamori A, Nakamura M, Tomioka M, Kawaka Y, Yamada Y, Negi A. Agreement among three types of spectral-domain optical coherent tomography instruments in measuring parapapillary retinal nerve fibre layer thickness. Br J Ophthalmol. 2012;96:832–7.
15. Bland JM, Altman DG. Statistical methods for assessing agreement between two methods of clinical measurement. Lancet. 1986;1:307–10.
16. DeLong ER, DeLong DM, Clarke-Pearson DL. Comparing the areas under two or more correlated receiver operating characteristic curves: a nonparametric approach. Biometrics. 1988;44:837–45.
17. Stephan C, Wesseling S, Schink T, Jung K. Comparison of eight computer programs for receiver-operating characteristic analysis. Clin Chem. 2003;49:433–9.
18. Leung CK, Cheung CY, Weinreb RN, Qiu Q, Liu S, Li H, et al. Retinal nerve fiber layer imaging with spectral-domain optical coherence tomography: a variability and diagnostic performance study. Ophthalmology. 2009;116:1257–63.

19. Park SB, Sung KR, Kang SY, Kim KR, Kook MS. Comparison of glaucoma diagnostic capabilities of Cirrus HD and Stratus optical coherence tomography. Arch Ophthalmol. 2009;127:1603–9.
20. Lee S, Sung KR, Cho JW, Cheon MH, Kang SY, Kook MS. Spectral-domain optical coherence tomography and scanning laser polarimetry in glaucoma diagnosis. Jpn J Ophthalmol. 2010;54:544–9.
21. Kanamori A, Nakamura M, Tabuchi K, Yamada Y, Negi A. Effects of ocular rotation on parapapillary retinal nerve fiber layer thickness analysis measured with spectral-domain optical coherence tomography. Jpn J Ophthalmol. 2012;56:354–61.
22. Kotera Y, Hangai M, Hirose F, Mori S, Yoshimura N. Three-dimensional imaging of macular inner structures in glaucoma by using spectral-domain optical coherence tomography. Invest Ophthalmol Vis Sci. 2011;52:1412–21.
23. Leite MT, Rao HL, Weinreb RN, Zangwill LM, Bowd C, Sample PA, et al. Agreement among spectral-domain optical coherence tomography instruments for assessing retinal nerve fiber layer thickness. Am J Ophthalmol. 2011;151:85–92.
24. Huang J, Liu X, Wu Z, Guo X, Xu H, Dustin L, et al. Macular and retinal nerve fiber layer thickness measurements in normal eyes with the Stratus OCT, the Cirrus HD-OCT, and the Topcon 3D OCT-1000. J Glaucoma. 2011;20:118–25.
25. Tuulonen A, Airaksinen PJ. Initial glaucomatous optic disk and retinal nerve fiber layer abnormalities and their progression. Am J Ophthalmol. 1991;111:485–90.